Molecular Cell, Vol. 18, 61–69, April 1, 2005, Copyright ©2005 by Elsevier Inc. DOI 10.1016/j.molcel.2005.02.033

Cyclic ADP-Ribose and Hydrogen Peroxide Synergize with ADP-Ribose in the Activation of TRPM2 Channels

Martin Kolisek,[1,2] Andreas Beck,[1,2] Andrea Fleig,[1] and Reinhold Penner[1,*]
[1]Laboratory of Cell and Molecular Signaling
Center for Biomedical Research
The Queen's Medical Center
John A. Burns School of Medicine
University of Hawaii
Honolulu, Hawaii 96813

Summary

The melastatin-related transient receptor potential channel TRPM2 is a plasma membrane Ca^{2+}-permeable cation channel that is activated by intracellular adenosine diphosphoribose (ADPR) binding to the channel's enzymatic Nudix domain. Channel activity is also seen with nicotinamide dinucleotide (NAD^+) and hydrogen peroxide (H_2O_2), but their mechanisms of action remain unknown. Here, we identify cyclic adenosine diphosphoribose (cADPR) as an agonist of TRPM2 with dual activity: at concentrations above 100 μM, cADPR can gate the channel by itself, whereas lower concentrations of 10 μM have a potentiating effect that enables ADPR to gate the channel at nanomolar concentrations. ADPR's breakdown product adenosine monophosphate (AMP) specifically inhibits ADPR, but not cADPR-mediated gating of TRPM2, whereas the cADPR antagonist 8-Br-cADPR exhibits the reverse block specificity. Our results establish TRPM2 as a coincidence detector for ADPR and cADPR signaling and provide a functional context for cADPR as a second messenger for Ca^{2+} influx.

Introduction

The TRPM2 ion channel, previously named TRPC7 (Nagamine et al., 1998) or LTRPC2 (Perraud et al., 2001; Sano et al., 2001) and recently designated TRPM2 for melastatin-related transient recptor potential channel 2 (Montell et al., 2002), has been shown to be a nonselective cation channel specifically gated by ADPR (Perraud et al., 2001; Sano et al., 2001). Intracellular Ca^{2+} appears to be an important modulator and cofactor of TRPM2, as elevated $[Ca^{2+}]i$ can significantly increase the sensitivity of TRPM2 toward ADPR, enabling the nucleotide to gate the channel at lower concentrations (Perraud et al., 2001; McHugh et al., 2003). The channel can also be gated by H_2O_2 (Hara et al., 2002) and NAD^+ (Sano et al., 2001; Hara et al., 2002; Heiner et al., 2003). The mechanism of H_2O_2-mediated gating of TRPM2 has been proposed to be direct and independent of NAD^+ or ADPR (Wehage et al., 2002) as well as indirect via conversion of NADH to NAD^+ (Hara et al., 2002). More recent evidence suggests an indirect mechanism, because H_2O_2 releases ADPR from mitochondria (Perraud et al., 2005), and its ability to activate TRPM2 is lost when mutating the ADPR binding site (Kuhn and Luckhoff, 2004). The mechanism by which NAD^+ mediates activation of TRPM2 remains uncertain. This precursor of ADPR can also gate TRPM2 in both whole-cell recordings and excised membrane patches (Sano et al., 2001; Hara et al., 2002); however, this requires very high concentrations of 1 mM NAD^+ and even then proceeds after long delays. It is neither clear whether this effect has physiological relevance nor whether it occurs via the highly specific ADPR binding site in the channel's Nudix domain.

Although TRPM2 is dominantly expressed in the brain, it is also detected in many other tissues, including bone marrow, spleen, heart, leukocytes, liver, and lung. Native TRPM2 currents have been recorded from the U937 monocyte cell line (Perraud et al., 2001), neutrophils (Heiner et al., 2003), microglia (Kraft et al., 2004), and CRI-G1 insulinoma cells (Inamura et al., 2003) where ADPR induces large cation currents (designated I_{ADPR}) that closely match those mediated by heterologously expressed TRPM2. Interestingly, many of the cell types in which TRPM2 is expressed (e.g., lymphocytes, neutrophils, and pancreatic β cells) have also been reported to utilize cADPR as a second messenger for Ca^{2+} signaling—cADPR is thought to function as an endogenous regulator of Ca^{2+}-induced Ca^{2+} release via ryanodine receptors (for reviews see Dousa et al. [1996], Lund et al. [1998], Lee et al. [1999], Galione and Churchill [2000], Lee [2000b], Galione and Churchill [2002], and Guse [2002]). Recent evidence has indicated that cADPR may also be involved in Ca^{2+} influx (Guse et al., 1997; Guse et al., 1999; Partida-Sanchez et al., 2001), although it is not clear whether this effect is indirect through Ca^{2+} release and subsequent activation of store-operated channels or through cADPR metabolites or more directly via cADPR-activated cation channels. Based on the crystal structure of the human ADPR pyrophosphatase NUDT9, which is highly homologous to the ADPR binding C-terminal enzymatic domain of TRPM2 (Shen et al., 2003) and provides a highly specific binding site for ADPR, it seems unlikely that the rather different molecular structures of either NAD^+ or cADPR may be able to bind to that domain and gate the channel in lieu of ADPR.

ADPR is part of a complex metabolic network (see Figure 1) that lies downstream of NAD^+. NAD^+ is a substrate of CD38, a multifunctional ectoenzyme with activities of ADP-ribosyl cyclase, cyclic ADPR hydrolase, and NAD^+ glycohydrolase that can generate both ADPR and cADPR. cADPR can be further converted to ADPR by the same enzyme. CD38 is expressed in a wide range of cells and tissues and involved in growth and differentiation signaling of lymphoid and myeloid cells (Funaro and Malavasi, 1999; Lee, 2000a; Schuber and Lund, 2004). Many of these cells also express TRPM2, indicating that CD38 signaling may be linked to TRPM2 channel activity. In addition to CD38 and the CD38-like enzyme BST-1/CD157, several other less well-characterized enzymes are involved in NAD^+, cADPR, and

*Correspondence: rpenner@hawaii.edu
[2]These authors contributed equally to this work.

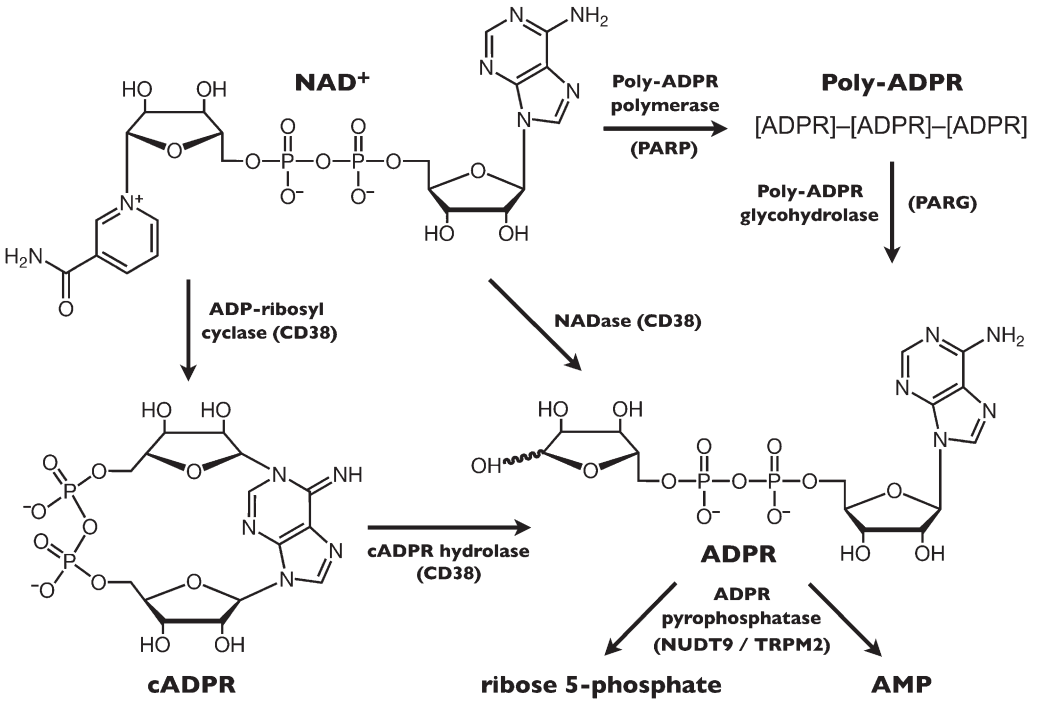

Figure 1. Metabolic Pathways of NAD^+, ADPR, and cADPR

Two-dimensional chemical structures of NAD^+, ADPR, and cADPR and enzymes responsible for their metabolism.

ADPR metabolism, including NAD^+ glycohydrolases, ADP-ribosyl transferases, and ADP-ribosyl cyclases. Another source for ADPR is found in polymeric ADPR, which is complexed by the poly-ADPR polymerase PARP and hydrolyzed by the poly-ADPR glycohydrolase PARG (Davidovic et al., 2001; Soldani and Scovassi, 2002; Fonfria et al., 2004). This mechanism is invoked in the context of DNA damage and repair, and excessive production of ADPR could link TRPM2 activation to apoptotic cell death. ADPR itself is subject to enzymatic breakdown into AMP and ribose 5-phosphate by TRPM2's endogenous Nudix domain as well as a closely related ADPR pyrophosphatase, NUDT9 (Perraud et al., 2001; Shen et al., 2003).

The present study was aimed at elucidating the role of the molecules in the metabolic network surrounding ADPR on the functional properties of TRPM2 ion channels. Here, we report that ADPR and cADPR can activate TRPM2 directly via independent gating mechanisms. Importantly, both agonists synergize with each other and dramatically reduce each others' effective concentration required to gate the channel. In addition, we demonstrate that one of the breakdown products of ADPR, AMP, exerts a potent negative feedback inhibition on TRPM2 activity.

Results

To assess the efficacy and characteristics of the various molecules in the metabolic network surrounding ADPR, HEK-293 cells stably expressing TRPM2 under a tetracycline-inducible promoter were perfused intracellularly with various concentrations of ADPR, NAD^+, cADPR, and H_2O_2 (Figure 2). We chose experimental conditions in which the ionic composition of extra- and intracellular solutions were kept as close as possible to physiological conditions, i.e., extracellular solutions were NaCl based with 1 mM Ca^{2+} and 2 mM Mg^{2+}, whereas intracellular solutions were K-glutamate based and contained 8 mM NaCl and 1 mM Mg^{2+} without added Ca^{2+} buffers. Within seconds, ADPR caused the activation of large linear currents with the typical characteristics of TRPM2 (Figures 2A and 2F). ADPR-induced current activation was dose dependent with a half-maximal effective concentration (EC_{50}) of 12 μM (Figure 2E). At high concentrations of ADPR, currents peaked very rapidly, reaching ~17 nA at –80 mV. ADPR's precursor, NAD^+, also activated large linear currents (Figures 2B and 2F), but it was less potent and had about a 100-fold higher EC_{50} of ~1 mM (Figure 2E). In contrast to the immediate onset of ADPR-induced currents, TRPM2 activation by NAD^+ was characterized by a significant delay of 50–150 s (Figure 2B).

Intracellular perfusion of cells with H_2O_2 also activated linear currents in a dose-dependent manner (Figures 2C and 2F), but in contrast to ADPR and NAD^+, H_2O_2 induced only modest increases in current well below 1 nA. The EC_{50} for H_2O_2 was ~50 μM (Figure 2E); however, assessment of the dose-response curve for H_2O_2 was limited to concentrations up to 200 μM, because higher concentrations were not tolerated by cells and resulted in seal breakdown. The seal breakdown was easily distinguished from the smoothly developing TRPM2 currents, because it manifested itself by abrupt

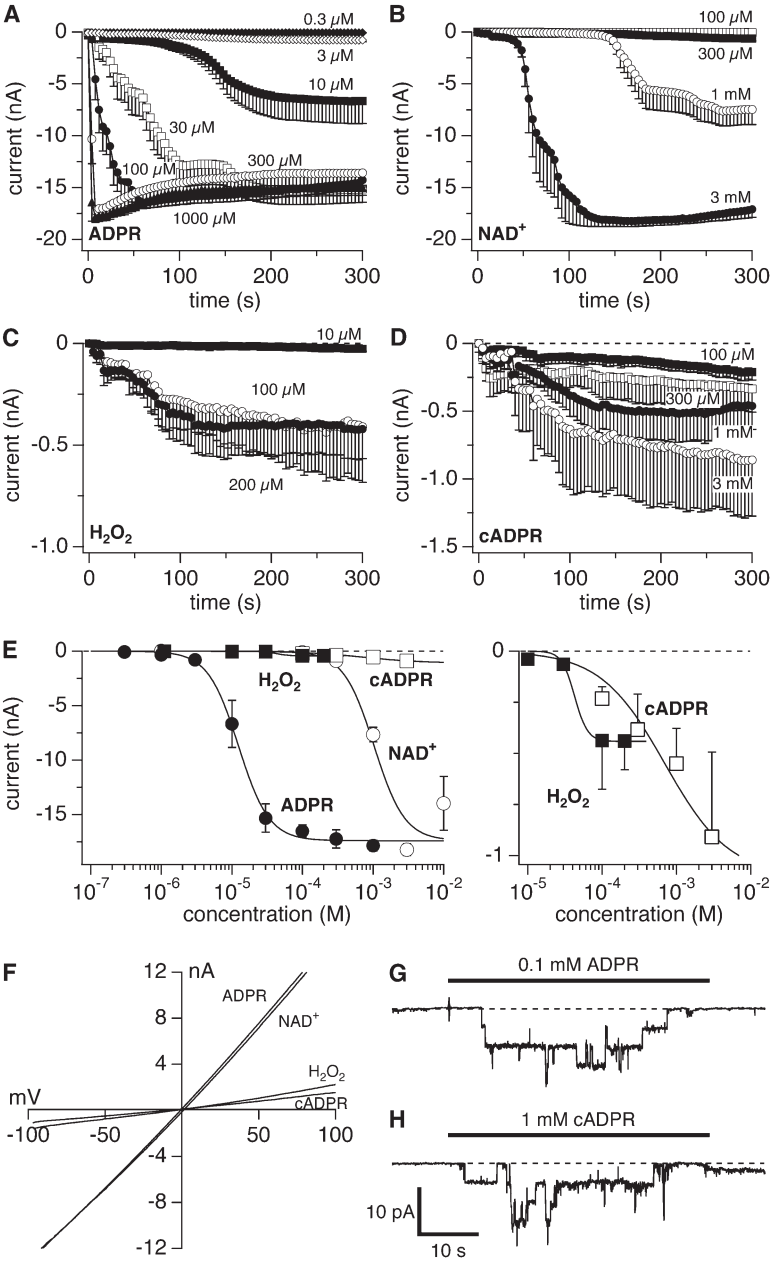

Figure 2. ADPR, NAD^+, H_2O_2, and cADPR Activate TRPM2 Channels

Tetracycline-induced HEK-293 cells (1 μg/ml, 15 hr) expressing TRPM2 were perfused with K-glutamate-based pipette solutions without added Ca^{2+} buffers containing ADPR, NAD^+, H_2O_2, and cADPR at various concentrations.

(A–D) Average membrane currents (±SEM) recorded at –80 mV induced by perfusion of cells with various concentrations of ADPR (n = 6–13), NAD^+ (n = 3–10), H_2O_2 (n = 4–10), and cADPR (n = 4–7).

(E) Dose-response curves for ADPR (EC_{50} = 12 μM, Hill coefficient = 2), NAD^+ (EC_{50} = 1 mM, Hill coefficient = 2), H_2O_2 (EC_{50} = 50 μM, Hill coefficient = 4), and cADPR (EC_{50} = 700 μM, Hill coefficient = 1). Data points reflect average peak currents (±SEM) recorded at –80 mV (n = 3–13). The right panel depicts enlarged dose-response curves for H_2O_2 and cADPR.

(F) Typical current-voltage (I-V) relationships of TRPM2 whole-cell currents induced by ADPR, NAD^+, H_2O_2, and cADPR. I-V curves were derived from voltage ramps taken from representative cells.

(G and H) Examples of single-channel activity in excised membrane patches held at –80 mV and exposed to 100 μM ADPR or 1 mM cADPR for the time indicated by the bar.

and erratic increases in linear leak currents that often exceeded the typical maximal currents induced by ADPR. Finally, we tested cADPR and found that it too activated linear currents (Figures 2D and 2F) in a similar manner as H_2O_2. Activation was dose dependent (Figure 2E) with an EC_{50} of 700 μM. As with H_2O_2, the cADPR-induced currents were typically rather small. On some rare occasions, we encountered cells in which cADPR elicited currents in excess of 10 nA, and we attribute this to elevated basal levels of ADPR (see below). Neither of the agonists elicited any significant currents in wild-type HEK-293 cells or in noninduced cells (TRPM2-transfected cells that were not exposed to tetracycline). It should also be noted that only ADPR was capable of activating TRPM2 currents when $[Ca^{2+}]i$ was clamped to very low levels with 10 mM BAPTA—maximal NAD^+, cADPR, and H_2O_2 were completely ineffective in activating any TRPM2 currents under these conditions (data not shown).

These results suggest that all four agonists, ADPR, NAD^+, cADPR, and H_2O_2, are capable of activating TRPM2. However, they do so with varying degrees of potency and also exhibit differences in kinetics of activation, indicating that they might act through different mechanisms and/or through metabolic conversions. In terms of kinetics of activation, ADPR was clearly the fastest of the four agonists, suggesting a direct activation of TRPM2 channels and being consistent with its binding to the Nudix domain (Perraud et al., 2001; Kuhn and Luckhoff, 2004). The marked delay of TRPM2 acti-

vation observed with NAD^+ might indicate that its effect is not direct and possibly due to ADPR contamination and/or secondary to metabolic conversion to ADPR. Given the fact ADPR is about two orders of magnitude more potent than NAD^+, the ADPR contamination of 2.9% in our lot of NAD^+ (see Experimental Procedures) likely accounts for the observed effects. The two other agonists, cADPR and H_2O_2, had intermediate kinetics so that peak currents were attained after 100–200 s. In addition, maximal currents induced by these stimuli usually remained below 5% of those typically achieved by ADPR. This would suggest that cADPR and H_2O_2 may gate TRPM2 directly, but their efficacy appears too low to bear physiological significance.

To assess whether the effects of cADPR were secondary to intracellular metabolism, we performed single-channel recordings in excised membrane patches where such conversion would likely be absent. Consistent with the small cADPR-mediated, whole-cell currents, it proved difficult to obtain cADPR-induced, single-channel activity in excised membrane patches. Only one out of eight membrane patches exposed to 1 mM cADPR induced multichannel openings with the typical long open times of TRPM2 (Figure 2H). All other patches were either silent or showed only rare channel activity with brief openings. In contrast, 100 μM ADPR reliably (eight out of 12 patches) caused multichannel activity of up to 16 channels per patch (Figure 2G). Because HPLC analysis of our cADPR lot did not reveal ADPR as an appreciable contaminant, these data would suggest that cADPR has some limited capability to gate TRPM2 channels directly.

Because ADPR is subject to metabolic breakdown into ribose 5-phosphate and AMP, we tested for possible effects of these two metabolites on ADPR-mediated activation of TRPM2. Consistent with our previous findings (Perraud et al., 2001), neither of the two metabolites activated TRPM2 at concentrations up to 1 mM (data not shown). We also found no obvious inhibitory effect of ribose 5-phosphate (100 μM) on TRPM2 currents induced by 30 μM ADPR (Figure 3A). In contrast, AMP exhibited a potent dose-dependent inhibition of ADPR-induced currents (Figure 3B), where 100 μM AMP caused ~70% inhibition, and 300 μM AMP essentially abolished any current response to 100 μM ADPR. The dose-response relationship of this inhibitory effect is illustrated in Figure 3C, and the fit to these data yielded an IC_{50} of ~70 μM. The antagonistic action of AMP allowed us to test whether it affected any of the other agonists. Figure 3D illustrates that 500 μM AMP also completely suppressed TRPM2 activation by 1 mM NAD^+ (or its ADPR contaminant). However, the same concentration of AMP was ineffective at antagonizing the small currents evoked by either 1 mM cADPR (Figure 3E) or 100 μM H_2O_2 (Figure 3F), which implies that the inhibition is specific for the agonist and not due to a simple block of the channel. These results therefore indicate that the ADPR-mediated TRPM2 activation mechanism is susceptible to AMP inhibition and distinct from the AMP-insensitive channel activity induced by cADPR or H_2O_2.

Previous work has established 8-Br-cADPR as a selective and potent antagonist of cADPR-mediated Ca^{2+} signaling (Walseth and Lee, 1993), prompting us to test this molecule for possible antagonism on TRPM2 activation by the various agonists. When perfusing cells intracellularly with 100 μM of 8-Br-cADPR along with 1 mM cADPR, the compound indeed completely suppressed TRPM2 activation by cADPR (Figure 4A). Likewise, 8-Br-cADPR completely suppressed the H_2O_2-mediated activation of TRPM2. However, 8-Br-cADPR did not suppress TRPM2 activation by either 100 μM ADPR (Figure 4C) or 1 mM NAD^+ (Figure 4D). This would suggest that both cADPR and H_2O_2 might activate TRPM2 through a common 8-Br-cADPR-sensitive mechanism, whereas ADPR and NAD^+ activate TRPM2 independently through an AMP-sensitive, but 8-Br-cADPR-independent, mechanism.

As evident from Figures 4C and 4D, 8-Br-cADPR actually accelerated the kinetics of ADPR- and NAD^+-mediated activation of TRPM2, and we considered the possibility that the gating mechanisms of ADPR/NAD^+ and cADPR/H_2O_2 might involve some form of cooperativity or synergy. To test this, we stimulated cells with combinations of various agonists at concentrations that were below the threshold for activating TRPM2 when used individually. As illustrated in Figure 5A, the combination of 10 μM cADPR and various subthreshold concentrations of ADPR caused a strong activation of TRPM2 with an IC_{50} of 90 nM. Thus, the presence of cADPR caused a 100-fold shift in TRPM2's sensitivity to ADPR (Figure 5B), demonstrating that TRPM2 activity is synergistically enhanced when the channel binds two agonists. This synergy occurred over a narrow subthreshold concentration range of cADPR and ADPR, because lowering the concentration of either cADPR to 3 μM while maintaining ADPR at 300 nM (data not shown) or reducing ADPR to 10 nM while keeping cADPR at 10 μM was largely ineffective in triggering TRPM2 activity (Figure 5A). Disruption of this synergy by adding 500 μM AMP caused complete suppression of TRPM2 currents.

Because our previous experiments suggested that H_2O_2 behaves similarly to cADPR, we tested whether subthreshold concentrations of 10–30 μM H_2O_2 could synergize with 300 nM ADPR in a similar fashion as subtreshold levels of cADPR. At these subthreshold H_2O_2 concentrations, we did not observe significant potentiation (data not shown). However, increasing the H_2O_2 concentration to 100 μM, which by itself typically causes less than 5% of the maximal achievable TRPM2 current, induced large currents in excess of 15 nA at −80 mV even when the ADPR concentration was as low as 300 nM (Figure 5C). As in the case of combining cADPR and ADPR, addition of 500 μM AMP to the synergistic combination of H_2O_2 and ADPR completely suppressed activation of TRPM2. We also assessed the possible synergy of 10 μM cADPR and 300 μM NAD^+, which both represent ineffective concentrations when applied individually. As with ADPR, we observed a strong facilitation of TRPM2 activation (Figure 5D), yielding large currents that were almost identical to those observed with 1 mM NAD^+ alone. AMP proved effective in suppressing this effect. However, because we know that NAD^+ is contaminated with ADPR, these effects are likely attributable to the synergy of cADPR with ADPR rather than NAD^+.

A somewhat surprising aspect of the synergy be-

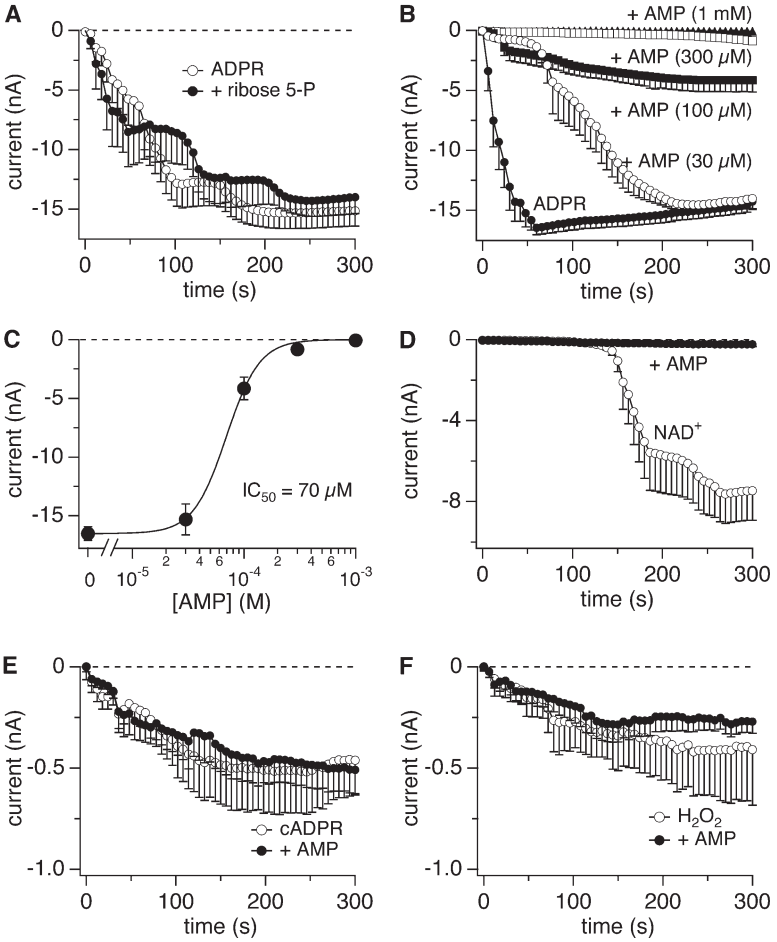

Figure 3. AMP Inhibits TRPM2 Gating by ADPR and NAD^+, but Not H_2O_2 and cADPR

(A) Average membrane currents (±SEM) recorded at –80 mV in cells perfused with 30 μM ADPR alone (n = 13) and in combination with its breakdown product ribose 5-phosphate (100 μM, n = 8).

(B) Average membrane currents (±SEM) recorded at –80 mV in cells perfused with 100 μM ADPR alone and in combination with various AMP concentrations (n = 4–8).

(C) Dose-response curve for AMP-dependent inhibition of TRPM2 currents activated by 100 μM ADPR. Data represent maximum average currents (±SEM) recorded at –80 mV and the dose-response fit yields an IC_{50} of 70 μM (Hill coefficient = 3).

(D) Average membrane currents (±SEM) recorded at –80 mV in cells perfused with 1 mM NAD^+ alone (n = 10) and in combination with 500 μM AMP (n = 5).

(E) Average membrane currents (±SEM) recorded at –80 mV in cells perfused with 1 mM cADPR alone (n = 4) and in combination with 500 μM AMP (n = 9).

(F) Average membrane currents (±SEM) recorded at –80 mV in cells perfused with 100 μM H_2O_2 alone (n = 10) and in combination with 500 μM AMP (n = 5).

tween cADPR and ADPR is that the cADPR antagonist 8-Br-cADPR also seems to enhance ADPR-mediated gating of TRPM2 (see Figures 4C and 4D). We assessed this in some more detail by perfusing cells with a subthreshold concentration of ADPR (3 μM) with increasing concentrations of 8-Br-cADPR. As illustrated in Figure

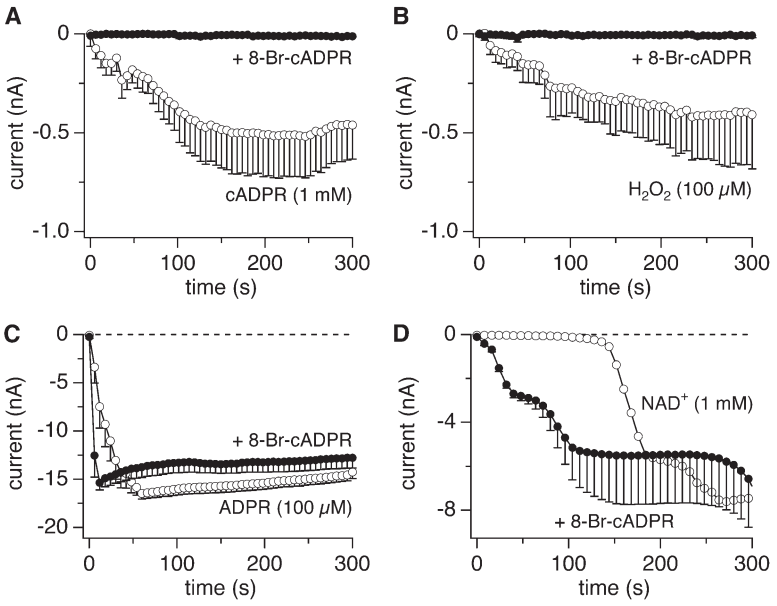

Figure 4. 8-Br-cADPR Inhibits TRPM2 Gating by cADPR and H_2O_2, but Not ADPR and NAD^+

(A) Average membrane currents (±SEM) recorded at –80 mV in cells perfused with 1 mM cADPR alone (n = 4) and in combination with 100 μM 8-Br-cADPR (n = 6).

(B) Average membrane currents (±SEM) recorded at –80 mV in cells perfused with 100 μM H_2O_2 alone (n = 10) and in combination with 100 μM 8-Br-cADPR (n = 7).

(C) Average membrane currents (±SEM) recorded at –80 mV in cells perfused with 100 μM ADPR alone (n = 7) and in combination with 100 μM 8-Br-cADPR (n = 6).

(D) Average membrane currents (±SEM) recorded at –80 mV in cells perfused with 1 mM NAD^+ alone (n = 10) and in combination with 100 μM 8-Br-cADPR (n = 8).

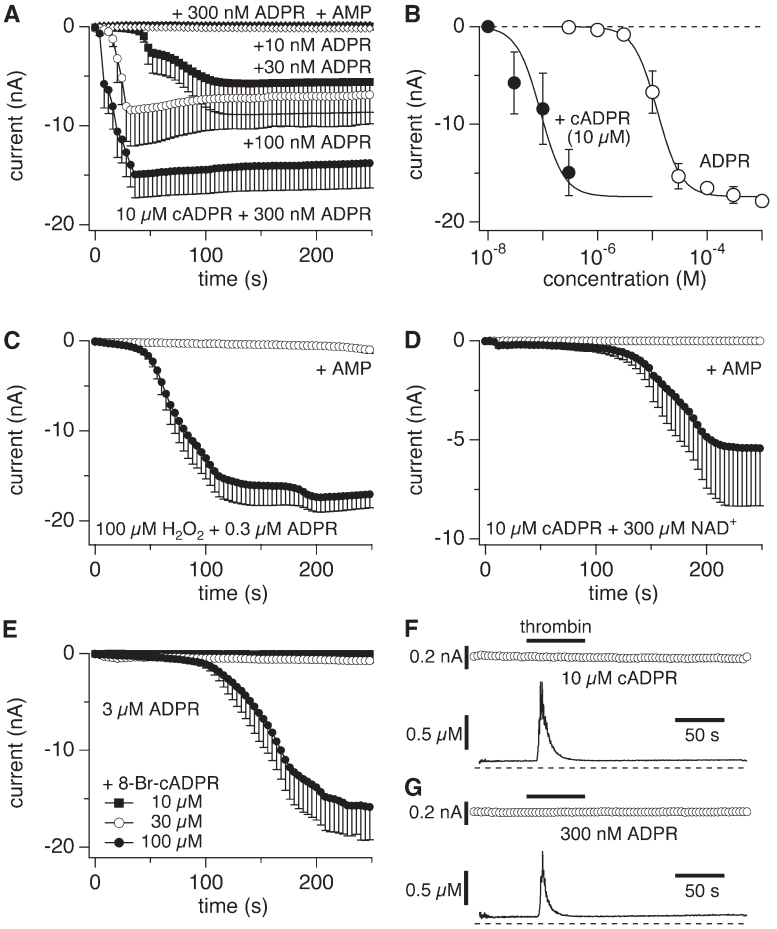

Figure 5. Subthreshold Concentrations of cADPR and H_2O_2 Potentiate TRPM2 Activation by Subthreshold Levels of ADPR and NAD^+

(A) Average membrane currents (±SEM) recorded at –80 mV in cells perfused with 10 μM cADPR in combination with various concentrations of ADPR (n = 4–7). This effect was blocked by addition of 500 μM AMP (n = 6).

(B) Dose-response curves for ADPR (EC_{50} = 12 μM, Hill coefficient = 2; taken from Figure 2F) and ADPR in combination with 10 μM cADPR (EC_{50} = 90 nM, Hill coefficient = 2). Data points reflect average peak currents (±SEM) recorded at –80 mV (n = 3–13).

(C) Average membrane currents (±SEM) recorded at –80 mV in cells perfused with 300 nM ADPR in combination with 100 μM H_2O_2 (n = 11). This effect was blocked by addition of 500 μM AMP (n = 8).

(D) Average membrane currents (±SEM) recorded at –80 mV in cells perfused with 300 μM NAD^+ in combination with 10 μM cADPR (n = 5). This effect was blocked by addition of 500 μM AMP (n = 6).

(E) Average membrane currents (±SEM) recorded at –80 mV in cells perfused with 3 μM ADPR in combination with various concentrations of 8-Br-cADPR (n = 4–8).

(F and G) Average membrane currents (±SEM) recorded at –80 mV and average $[Ca^{2+}]i$ signals in cells perfused with either 10 μM cADPR (n = 3) or 300 nM ADPR (n = 5). In both experiments, thrombin (20 U/ml) was applied at the time indicated by the bar. Note that reliable fluorescence measurements start 6 s after whole-cell establishment.

5E, the threshold for the potentiation of ADPR by 8-Br-cADPR is around 100 μM, making it about ten times less potent than cADPR. Although the potentiation by 8-Br-cADPR was observed in most cells across multiple preparations, we encountered two preparations in which the potentiation was not obvious even at higher concentrations of 8-Br-cADPR, indicating that the potentiating effect of 8-Br-cADPR might not be as robust as that of cADPR. Although our lot of 8-Br-cADPR contained about 4% of Br-ADPR, this contaminant does not appear to act like ADPR, because 300 μM 8-Br-cADPR (with a Br-ADPR contamination of 12 μM) did not cause any TRPM2 activation (data not shown). Thus, 8-Br-cADPR has a dual effect in that it inhibits cADPR- and H_2O_2-mediated gating of TRPM2 but at the same time can mimic their effects in synergizing with ADPR. This behavior is typical of a partial agonist.

Because one of the established mechanisms of cADPR, at least in some cell types, encompasses Ca^{2+} release from intracellular stores and because elevated $[Ca^{2+}]i$ enhances TRPM2's sensitivity to ADPR, we tested whether the cADPR-mediated potentiation was somehow related to Ca^{2+} release. In combined whole-cell patch-clamp and fura-2 measurements, we perfused TRPM2-expressing HEK-293 cells with 10 μM cADPR alone (Figure 5F). As expected, cADPR neither activated TRPM2 currents nor did it seem to cause a substantial increase in $[Ca^{2+}]i$. Although the fura-2 concentration in the initial 6 s after establishing the whole-cell configuration is too low to permit an accurate assessment of $[Ca^{2+}]i$, any Ca^{2+} release induced by cADPR would have to be very brief, because just 6 s into the experiment, $[Ca^{2+}]i$ was at resting levels, and subsequent stimulation of $InsP_3$-mediated release by thrombin occurred normally (Figure 5F). To further rule out changes in $[Ca^{2+}]i$ as the mechanism of cADPR-mediated potentiation, we perfused cells with 300 nM ADPR and again stimulated cells with thrombin to elicit Ca^{2+} release (Figure 5G). However, the large $InsP_3$-mediated Ca^{2+} release transients did not cause TRPM2 activation and therefore failed to synergize with 300 nM ADPR, a concentration at which cADPR fully potentiates TRPM2 activation. Thus, we conclude that the cADPR-mediated potentiation effect is not rooted in a possible Ca^{2+} release mechanism.

Discussion

Previous work on the TRPM2 ion channel has established that channel activity can be induced by ADPR, NAD^+, and H_2O_2. The present study adds several new facets to the complex gating mechanisms of TRPM2 in that it establishes cADPR as an agonist for this channel

and AMP as a negative feedback regulator. Several lines of evidence suggest that ADPR may be the primary direct agonist for TRPM2. The molecule binds with high specificity to the channel's Nudix domain (Perraud et al., 2001; Sano et al., 2001; Shen et al., 2003; Kuhn and Luckhoff, 2004), it causes rapid and full activation of TRPM2 in whole-cell recordings (Perraud et al., 2001; Sano et al., 2001), and it gates the channel in excised membrane patches (Perraud et al., 2001). In the present study, we used a more physiological K-glutamate-based intracellular solution in which Ca^{2+} was not buffered by chelators so that $[Ca^{2+}]i$ could vary freely. Because Ca^{2+} facilitates the gating of TRPM2 channels (Perraud et al., 2001; McHugh et al., 2003), we observed very fast ADPR-mediated activation of currents in excess of 15 nA at –80 mV at 1 mM ADPR. At lower concentrations, the TRPM2 currents activated more slowly, and at ~10 μM, the current amplitudes were also reduced. Because our lot of ADPR was relatively pure (99.1%), the EC_{50} of 12 μM obtained under these experimental conditions is likely accurate.

The gating of TRPM2 by NAD^+ seems more complex, because the activation of whole-cell currents is characterized by a long delay ([Sano et al., 2001; Hara et al., 2002], see Figure 2B) or is not observed at all even at high concentrations (Wehage et al., 2002). In addition, current structural information about the ADPR binding site in the channel's Nudix domain suggests a high selectivity for ADPR (Perraud et al., 2001; Shen et al., 2003) that would not easily accommodate the binding of the structurally quite distinct NAD^+ molecule, further suggesting that NAD^+ might have an indirect mechanism of action. However, because some studies observed relatively fast activation of NAD^+-dependent channel activity in excised membrane patches (Sano et al., 2001; Hara et al., 2002), it has been proposed that NAD^+ is a direct activator of TRPM2, and the delay in whole-cell recordings might be due to an inhibitory effect of intracellular ATP so that current activation starts only after cellular ATP levels decrease (Sano et al., 2001). Another study has not observed the inhibitory effect of ATP (Hara et al., 2002), and we also failed to detect any obvious suppression of NAD^+-activated currents in the presence of 3 mM Mg·ATP (our unpublished data). The results from the present study may resolve some of the conflicting observations, as they suggest that the effects of NAD^+ are likely rooted in ADPR contaminations. When considering the 100-fold higher EC_{50} of NAD^+ relative to ADPR, a contamination of commercial samples of NAD^+ with just 1% ADPR would fully account for the effects observed with NAD^+ (based on the manufacturer's HPLC analysis, our lot of NAD^+ contained 2.8% ADPR). Consistent with this, we note the striking similarity of TRPM2 current activation observed with 1 mM NAD^+ and 10 μM ADPR (cf. Figures 2A and 2B).

The cADPR-mediated activation of TRPM2 appears to result from a direct gating mechanism, because TRPM2 activation by cADPR was relatively rapid in whole-cell recordings (see Figure 2D), and the compound triggered single-channel activity in excised membrane patches. However, these effects are not likely to be of significant physiological relevance, as they require relatively high concentrations of cADPR and even then the maximal current amplitude is rather limited, amounting to less than 5% of the maximal amplitude attainable with ADPR. However, when combined with ADPR or NAD^+, cADPR strongly potentiates TRPM2 activation. The direct cADPR-mediated gating of TRPM2 can be suppressed by 8-Br-cADPR, whereas the synergistic activation by subthreshold combinations of cADPR and ADPR can be disrupted by AMP. Considering that 30 nM ADPR in combination with 10 μM cADPR already yielded several nanoamperes of TRPM2 current (see Figure 5A) and that even 1 mM cADPR produced only about 0.5 nA of current (see Figure 2D), we must assume that virtually no contaminating ADPR is present in our cADPR sample. From this, we can also conclude that the cADPR-induced, single-channel activity observed in excised membrane patches is likely caused by a direct gating mechanism.

Our results obtained with 8-Br-ADPR do not seem to reflect a simple competitive antagonism to cADPR, because 8-Br-cADPR exhibits a dual mode of action. With respect to the direct activation of TRPM2 by cADPR, 8-Br-cADPR acts as a competitive antagonist, presumably by binding with high affinity to the cADPR binding site. As a result, even high concentrations of cADPR can no longer activate TRPM2 directly. However, 8-Br-cADPR has a second effect in that it appears to potentiate ADPR-mediated gating of TRPM2 similar to cADPR. In that function, it acts as an agonist, but with lower efficacy compared to cADPR, because it requires at least 100 μM 8-Br-cADPR. Thus, 8-Br-cADPR exhibits the features of a partial agonist.

Previously published data indicate that TRPM2 can also be gated by H_2O_2 and it has been suggested to gate the channel independently of ADPR (Wehage et al., 2002); however, a more recent study by the same group failed to observe H_2O_2-dependent gating of TRPM2 when modifying the Nudix domain (Kuhn and Luckhoff, 2004). Because Scharenberg and colleagues recently demonstrated that reducing the ADPR concentration within mitochondria largely suppresses H_2O_2-mediated activation of TRPM2 (Perraud et al., 2005), it now appears that the gating mechanism of H_2O_2 is primarily based on its ability to release ADPR from mitochondria, which then proceed to activate TRPM2. Our present data add an interesting facet to this scenario, because they suggest that the effects of H_2O_2 are very similar, if not identical, to those of cADPR. Although H_2O_2 has only limited efficacy in activating TRPM2 directly, it can synergize with ADPR to potentiate TRPM2 activation. Thus, H_2O_2 might be a self-sufficient stimulus for TRPM2 activation, as it would initiate the release of ADPR from mitochondria and at the same time function as a potentiating cofactor of ADPR.

Our finding that cADPR can activate TRPM2 has important implications for cADPR function. Most studies propose that cADPR acts through the ryanodine receptor to release internal calcium stores. There is, however, some indication that cADPR may also play a role in calcium entry in some cell types. Thus, cADPR was found to induce Ca^{2+} influx in T cells by producing spikes of $[Ca^{2+}]i$ that were dependent on the presence of extracellular Ca^{2+} (Guse et al., 1997). In neutrophils stimulated by the bacterial chemoattractant, formyl-methionyl-leucyl-phenylalanine (fMLP), cyclic ADPR ap-

pears to be required for sustained extracellular Ca^{2+} influx, because Ca^{2+} influx in these cells is greatly reduced in transgenic mice that lack the ADP-ribosyl cyclase CD38 (Partida-Sanchez et al., 2001). The data presented here show that cADPR can regulate a plasma membrane ion channel in support of Ca^{2+} influx and may underlie the cADPR-mediated Ca^{2+} influx observed in some cell types. Whether cADPR ever reaches the high levels required to gate TRPM2 directly remains to be determined; however, at relatively low levels, it could well synergize with nanomolar concentrations of ADPR to activate TRPM2. This provides a context in which cADPR may function to support Ca^{2+} influx in cells that express TRPM2.

Experimental Procedures

Cells

Tetracycline-inducible HEK-293 Flag-TRPM2-expressing cells were cultured at 37°C with 5% CO_2 in DMEM supplemented with 10% fetal bovine serum. The medium was supplemented with blasticidin (5 μg/ml; Invitrogen) and zeocin (0.4 mg/ml; Invitrogen). Cells were resuspended in medium containing 1 μg/ml tetracycline (Invitrogen) 15 hr before experiments.

Solutions and Chemicals

For patch-clamp experiments, cells were kept in standard extracellular saline (in mM): 140 NaCl, 2.8 KCl, 1 $CaCl_2$, 2 $MgCl_2$, 10 glucose, and 10 HEPES·NaOH ([pH 7.2] adjusted with NaOH). Standard pipette-filling solutions contained (in mM): 140 K-glutamate, 8 NaCl, 1 $MgCl_2$, and 10 HEPES·KOH ([pH 7.2] adjusted with KOH). In some experiments, $[Ca^{2+}]i$ was buffered to very low levels with 10 mM BAPTA. All reagents were purchased from Sigma and dissolved in standard intracellular solution. HPLC analyses provided by the manufacturer determined the purity and major contaminants of the various nucleotides as follows: ADPR 99.1% (NAD^+ 0.3%), NAD^+ 94.8% (ADPR 2.9%, AMP 1.1%), cADPR 94.5% (NAD^+ and/or nicotinamide 4.2%), and 8-Br-cADPR 93.6% (Br-ADPR 5.1%).

Electrophysiology

Patch-clamp experiments were performed in the whole-cell configuration at 21–25°C. Data were acquired with Pulse software controlling an EPC-9 amplifier (HEKA, Lambrecht, Germany). Voltage ramps of 50 ms spanning the voltage range from −100 to +100 mV were delivered from a holding potential of 0 mV at a rate of 0.5 Hz over a period of 200–600 s. When applicable, voltages were corrected for liquid junction potentials. Currents were filtered at 2.9 kHz and digitized at 100 μs intervals. Capacitive currents and series resistance were determined and corrected before each voltage ramp. For analysis, the very first ramps before activating the currents were digitally filtered at 2 kHz, pooled, and used for leak subtraction of all subsequent current records. The low-resolution temporal development of currents for a given potential was extracted from the leak-corrected individual ramp current records by measuring the current amplitudes at voltages of −80 mV or +80 mV. Single channels were recorded from excised membrane patches in the inside-out configuration at −80 mV by using patch pipettes that were filled with standard saline. Cells were bathed in a nominally Ca^{2+}-free standard saline into which patches were initially excised. To stimulate channel activity, the inside of the patch was exposed to our standard intracellular solution supplemented with either ADPR or cADPR. Currents were filtered at 2.9 kHz and digitized at 100 μs intervals. For display purposes, data records were digitally filtered and downsampled to 100 Hz. All averaged current data sets represent the means of n determinations ± standard error of the mean (SEM.).

Fluorescence Measurements

In some experiments, the cytosolic calcium concentration of individual patch-clamped cells was monitored by including 100 μM fura-2 in the standard intracellular solution. Fluorescence signals were sampled at a rate of 5 Hz with a photomultiplier-based system using a monochromatic light source tuned to excite fura-2 fluorescence at 360 and 390 nm for 20 ms each (TILL Photonics, Gräfelfing, Germany). Emission was detected at 450–550 nm with a photomultiplier whose analog signals were sampled and processed by X-Chart software (HEKA, Lambrecht, Germany). Fluorescence ratios were translated into free intracellular calcium concentration based on calibration parameters derived from patch-clamp experiments with calibrated calcium concentrations. Local perfusion of individual cells with standard extracellular saline containing thrombin (20 U/ml) was achieved through a wide-tipped, pressure-controlled application pipette.

Acknowledgments

We thank Mahealani K. Monteilh-Zoller and Ka'ohimanu L. Dang for expert technical assistance and John G. Starkus for sharing information and discussing experimental data. This work was supported in part by the following grants from the National Institutes of Health: R01-NS40927, R01-AI50200, and R01-GM 063954 to R.P. and R01-GM 65360 to A.F.

Received: December 17, 2004
Revised: February 1, 2005
Accepted: February 28, 2005
Published: March 31, 2005

References

Davidovic, L., Vodenicharov, M., Affar, E.B., and Poirier, G.G. (2001). Importance of poly(ADP-ribose) glycohydrolase in the control of poly(ADP-ribose) metabolism. Exp. Cell Res. *268*, 7–13.

Dousa, T.P., Chini, E.N., and Beers, K.W. (1996). Adenine nucleotide diphosphates: emerging second messengers acting via intracellular Ca^{2+} release. Am. J. Physiol. *271*, C1007–C1024.

Fonfria, E., Marshall, I.C., Benham, C.D., Boyfield, I., Brown, J.D., Hill, K., Hughes, J.P., Skaper, S.D., and McNulty, S. (2004). TRPM2 channel opening in response to oxidative stress is dependent on activation of poly(ADP-ribose) polymerase. Br. J. Pharmacol. *143*, 186–192.

Funaro, A., and Malavasi, F. (1999). Human CD38, a surface receptor, an enzyme, an adhesion molecule and not a simple marker. J. Biol. Regul. Homeost. Agents *13*, 54–61.

Galione, A., and Churchill, G.C. (2000). Cyclic ADP ribose as a calcium-mobilizing messenger. Sci. STKE *2000*, PE1.

Galione, A., and Churchill, G.C. (2002). Interactions between calcium release pathways: multiple messengers and multiple stores. Cell Calcium *32*, 343–354.

Guse, A.H. (2002). Cyclic ADP-ribose (cADPR) and nicotinic acid adenine dinucleotide phosphate (NAADP): novel regulators of Ca^{2+}-signaling and cell function. Curr. Mol. Med. *2*, 273–282.

Guse, A.H., Berg, I., da Silva, C.P., Potter, B.V., and Mayr, G.W. (1997). Ca^{2+} entry induced by cyclic ADP-ribose in intact T-lymphocytes. J. Biol. Chem. *272*, 8546–8550.

Guse, A.H., da Silva, C.P., Berg, I., Skapenko, A.L., Weber, K., Heyer, P., Hohenegger, M., Ashamu, G.A., Schulze-Koops, H., Potter, B.V., and Mayr, G.W. (1999). Regulation of calcium signalling in T lymphocytes by the second messenger cyclic ADP-ribose. Nature *398*, 70–73.

Hara, Y., Wakamori, M., Ishii, M., Maeno, E., Nishida, M., Yoshida, T., Yamada, H., Shimizu, S., Mori, E., Kudoh, J., et al. (2002). LTRPC2 Ca^{2+}-permeable channel activated by changes in redox status confers susceptibility to cell death. Mol. Cell *9*, 163–173.

Heiner, I., Eisfeld, J., and Luckhoff, A. (2003). Role and regulation of TRP channels in neutrophil granulocytes. Cell Calcium *33*, 533–540.

Inamura, K., Sano, Y., Mochizuki, S., Yokoi, H., Miyake, A., Nozawa, K., Kitada, C., Matsushime, H., and Furuichi, K. (2003). Response to ADP-ribose by activation of TRPM2 in the CRI-G1 insulinoma cell line. J. Membr. Biol. *191*, 201–207.

Kraft, R., Grimm, C., Grosse, K., Hoffmann, A., Sauerbruch, S., Kettenmann, H., Schultz, G., and Harteneck, C. (2004). Hydrogen peroxide and ADP-ribose induce TRPM2-mediated calcium influx and cation currents in microglia. Am. J. Physiol. Cell Physiol. *286*, C129–C137.

Kuhn, F.J., and Luckhoff, A. (2004). Sites of the NUDT9-H domain critical for ADP-ribose activation of the cation channel TRPM2. J. Biol. Chem. *279*, 46431–46437.

Lee, H.C. (2000a). Enzymatic functions and structures of CD38 and homologs. Chem. Immunol. *75*, 39–59.

Lee, H.C. (2000b). Multiple calcium stores: separate but interacting. Sci. STKE *2000*, PE1.

Lee, H.C., Munshi, C., and Graeff, R. (1999). Structures and activities of cyclic ADP-ribose, NAADP and their metabolic enzymes. Mol. Cell. Biochem. *193*, 89–98.

Lund, F.E., Cockayne, D.A., Randall, T.D., Solvason, N., Schuber, F., and Howard, M.C. (1998). CD38: a new paradigm in lymphocyte activation and signal transduction. Immunol. Rev. *161*, 79–93.

McHugh, D., Flemming, R., Xu, S.Z., Perraud, A.L., and Beech, D.J. (2003). Critical intracellular Ca^{2+} dependence of transient receptor potential melastatin 2 (TRPM2) cation channel activation. J. Biol. Chem. *278*, 11002–11006.

Montell, C., Birnbaumer, L., Flockerzi, V., Bindels, R.J., Bruford, E.A., Caterina, M.J., Clapham, D.E., Harteneck, C., Heller, S., Julius, D., et al. (2002). A unified nomenclature for the superfamily of TRP cation channels. Mol. Cell *9*, 229–231.

Nagamine, K., Kudoh, J., Minoshima, S., Kawasaki, K., Asakawa, S., Ito, F., and Shimizu, N. (1998). Molecular cloning of a novel putative Ca^{2+} channel protein (TRPC7) highly expressed in brain. Genomics *54*, 124–131.

Partida-Sanchez, S., Cockayne, D.A., Monard, S., Jacobson, E.L., Oppenheimer, N., Garvy, B., Kusser, K., Goodrich, S., Howard, M., Harmsen, A., et al. (2001). Cyclic ADP-ribose production by CD38 regulates intracellular calcium release, extracellular calcium influx and chemotaxis in neutrophils and is required for bacterial clearance in vivo. Nat. Med. *7*, 1209–1216.

Perraud, A.L., Fleig, A., Dunn, C.A., Bagley, L.A., Launay, P., Schmitz, C., Stokes, A.J., Zhu, Q., Bessman, M.J., Penner, R., et al. (2001). ADP-ribose gating of the calcium-permeable LTRPC2 channel revealed by Nudix motif homology. Nature *411*, 595–599.

Perraud, A.L., Takanishi, C.L., Shen, B., Kang, S., Smith, M.K., Schmitz, C., Knowles, H.M., Ferraris, D., Li, W., Zhang, J., et al. (2005). Accumulation of free ADP-ribose from mitochondria mediates oxidative stress-induced gating of TRPM2 cation channels. J. Biol. Chem. *280*, 6138–6148.

Sano, Y., Inamura, K., Miyake, A., Mochizuki, S., Yokoi, H., Matsushime, H., and Furuichi, K. (2001). Immunocyte Ca^{2+} influx system mediated by LTRPC2. Science *293*, 1327–1330.

Schuber, F., and Lund, F.E. (2004). Structure and enzymology of ADP-ribosyl cyclases: conserved enzymes that produce multiple calcium mobilizing metabolites. Curr. Mol. Med. *4*, 249–261.

Shen, B.W., Perraud, A.L., Scharenberg, A., and Stoddard, B.L. (2003). The crystal structure and mutational analysis of human NUDT9. J. Mol. Biol. *332*, 385–398.

Soldani, C., and Scovassi, A.I. (2002). Poly(ADP-ribose) polymerase-1 cleavage during apoptosis: an update. Apoptosis *7*, 321–328.

Walseth, T.F., and Lee, H.C. (1993). Synthesis and characterization of antagonists of cyclic-ADP-ribose-induced Ca^{2+} release. Biochim. Biophys. Acta *1178*, 235–242.

Wehage, E., Eisfeld, J., Heiner, I., Jungling, E., Zitt, C., and Luckhoff, A. (2002). Activation of the cation channel long transient receptor potential channel 2 (LTRPC2) by hydrogen peroxide. A splice variant reveals a mode of activation independent of ADP-ribose. J. Biol. Chem. *277*, 23150–23156.